Impact of an historic underground gas well blowout on the current methane chemistry in a shallow groundwater system

Gilian Schout[a,b,c,1], Niels Hartog[b,c], S. Majid Hassanizadeh[b], and Jasper Griffioen[a,d]

[a]Copernicus Institute of Sustainable Development, Utrecht University, 3584 CS Utrecht, The Netherlands; [b]Earth Sciences Department, Utrecht University, 3584 CD Utrecht, The Netherlands; [c]Geohydrology Unit, KWR Water Cycle Research Institute, 3433 PE Nieuwegein, The Netherlands; and [d]Geological Survey of the Netherlands, Nederlandse Organisatie voor Toegepast Natuurwetenschappelijk Onderzoek (TNO), 3584 CB Utrecht, The Netherlands

Edited by Susan L. Brantley, Pennsylvania State University, University Park, PA, and approved November 27, 2017 (received for review June 27, 2017)

Blowouts present a small but genuine risk when drilling into the deep subsurface and can have an immediate and significant impact on the surrounding environment. Nevertheless, studies that document their long-term impact are scarce. In 1965, a catastrophic underground blowout occurred during the drilling of a gas well in The Netherlands, which led to the uncontrolled release of large amounts of natural gas from the reservoir to the surface. In this study, the remaining impact on methane chemistry in the overlying aquifers was investigated. Methane concentrations higher than 10 mg/L ($n = 12$) were all found to have δ^{13}C-CH_4 values larger than −30‰, typical of a thermogenic origin. Both δ^{13}C-CH_4 and δD-CH_4 correspond to the isotopic composition of the gas reservoir. Based on analysis of local groundwater flow conditions, this methane is not a remnant but most likely the result of ongoing leakage from the reservoir as a result of the blowout. Progressive enrichment of both δ^{13}C-CH_4 and δD-CH_4 is observed with increasing distance and decreasing methane concentrations. The calculated isotopic fractionation factors of $\varepsilon_C = 3$ and $\varepsilon_D = 54$ suggest anaerobic methane oxidation is partly responsible for the observed decrease in concentrations. Elevated dissolved iron and manganese concentrations at the fringe of the methane plume show that oxidation is primarily mediated by the reduction of iron and manganese oxides. Combined, the data reveal the long-term impact that underground gas well blowouts may have on groundwater chemistry, as well as the important role of anaerobic oxidation in controlling the fate of dissolved methane.

groundwater contamination | well blowouts | methane | isotopic fingerprinting | anaerobic methane oxidation

Uncontrolled subsurface leaks of natural gas resulting from human underground activities have been shown to occur for several decades (1, 2). However, they became a highly debated subject in recent years after elevated methane concentrations in groundwater were attributed to well failure of nearby shale gas wells in an area of intense shale gas development (3–5). In addition to anthropogenically induced leaks of natural gas to groundwater, conduits for the migration of natural gas may exist naturally, as evidenced by phenomena such as methane seeps, mud volcanoes, and seabed pockmarks (6, 7). Leakage of natural gas through a freshwater aquifer can adversely affect groundwater quality by changing redox conditions and increasing pH (8, 9). Furthermore, it can result in an explosion and/or asphyxiation hazard (10).

Hydraulically induced fractures have also been investigated for their potential to act as conduits for gas leakage to groundwater (11). However, groundwater impacted by gas leakage through hydraulically induced fractures has never been unequivocally identified (12). In contrast, such connections are known to have been generated as a result of gas well blowouts (13). In general, blowouts occur during drilling when unexpectedly high gas pressures are encountered that can no longer be contained. While the frequency of blowouts is relatively low [~1:1,000 wells drilled (14)], their potential environmental impact is huge, as evident from high-profile cases such as the *Deepwater Horizon* (15) and Aliso Canyon (16) blowouts. In some cases, the pressures generated during a blowout do not escape at the surface but form a fracture network that allows the well to blow out underground (17). When these fractures reach the surface, they may negatively impact the chemistry of shallow groundwater by the massive introduction of methane (18).

In this study, we investigated the long-term effect of an underground blowout on the current methane chemistry in a shallow groundwater system. On December 1, 1965, an underground blowout with a catastrophic outcome occurred near the village of Sleen, The Netherlands. At a depth of 1,944 m below ground level, serious well control issues were experienced while drilling well SLN-02 (Fig. S1) as a result of an unexpectedly high downhole pressure. Eventually, gas started erupting from a crater that formed several tens of meters away from the spud point. Within 40 min (during which all personnel were evacuated), numerous similar eruptions appeared within a 350-m radius that coalesced to form a crater that engulfed the entire well pad. Half an hour later, the drilling rig collapsed and eventually sank completely into the ground (Fig. 1). On December 16, a relief well (SLN-03) was spudded ~600 m northwest of the blowout (Fig. S1). Using deviated drilling, this well was drilled toward the underground location of the blowout. At a depth of 1,924 m, hydraulic fracturing was successfully carried out to establish a connection with well SLN-02. On February 18, after more than 2.5 mo of near-continuous leakage of large amounts of natural gas, 760 m^3 of heavy mud, followed by 390 tons of cement, was injected into the relief well, which eventually caused the blowout to die out.

Significance

The rapid increase in shale gas production in recent years has led to increased attention to its potential negative environmental effects, including the risks of contaminating groundwater with methane and other substances. In this context, the uncontrolled gas migration that is triggered during well blowouts is an understudied environmental hazard. We show that the methane chemistry in shallow groundwater overlying the site of a catastrophic underground blowout continues to be impacted 50 y later. The occurrence of anaerobic methane oxidation limits the spatial extent to which the dissolved thermogenic methane plume could be observed and discerned from local biogenic methane sources. However, it also highlights the requirement to carry out monitoring in close proximity to potential gas leakage sources.

Author contributions: G.S., N.H., S.M.H., and J.G. designed research; G.S. performed research; G.S., N.H., S.M.H., and J.G. analyzed data; and G.S., N.H., and J.G. wrote the paper.

The authors declare no conflict of interest.

This article is a PNAS Direct Submission.

[1]To whom correspondence should be addressed. Email: g.schout@uu.nl.

This article contains supporting information online at www.pnas.org/lookup/suppl/doi:10.1073/pnas.1711472115/-/DCSupplemental.

Fig. 1. Aerial photograph (39) of the crater formed by the SLN-02 underground gas well blowout in 1965. Remnants of the well pad and associated trucks and trailers can be seen at the edge of the crater.

After the blowout, a network of groundwater monitoring wells was installed by the local drinking water production company to monitor for possible adverse effects on groundwater quality at the site of the blowout. For this study, we sampled all relevant monitoring wells. Samples were analyzed for dissolved gas molecular and isotopic composition as well as general groundwater chemistry. Aims of the study were to assess (*i*) the long-term effects of an underground gas well blowout on dissolved gas concentrations in the shallow aquifer, (*ii*) the fate of dissolved light hydrocarbons during groundwater transport, and (*iii*) secondary chemical effects of sustained elevated gas concentrations in groundwater.

Hydrogeological Setting

Currently, the site of the blowout is a small parcel of woodland entirely surrounded by pastures (Fig. 2). The topography is flat, with surface elevations of 16–18 m above sea level. The water table at the location of the blowout varies seasonally at between 1 and 2 m below ground surface. Based on head measurements in the monitoring wells near the blowout area (Fig. 2), the direction of groundwater flow is toward the south and east, with a low hydraulic gradient of roughly 0.25–0.50 m/km. The shallow geology is dominated by a thick succession of Quaternary sands and gravels down to a depth of around 120 m (Fig. 2). Three main formations are distinguished with increasing depth: the glacial Peelo Formation (fine- to medium-grained sand), the fluvial Appelscha Formation (coarse sand and gravel), and the marine Oosterhout Formation. The Oosterhout Formation consists of an upper unit of fine- to medium-grained sand and a lower unit that alternates sandy and clayey deposits. The Dutch National Hydrogeological Model, REGIS II (19), describes all but the lower Oosterhout clayey unit as having hydraulic conductivities between 10 and 100 $m \cdot d^{-1}$. The Oosterhout Formation is underlain by the highly impermeable Breda Formation, a clayey, marine, Neogene unit. Together with the aforementioned formations, it is part of the Upper North Sea Group, which extends to a depth of around 225 m (Fig. S1).

The Sleen gas field consists of a series of Triassic sand and claystone layers known together as the Main Bundsandstein Subgroup, part of the Lower Germanic Trias Group. Gas is capped in these layers by a more than 100-m-thick deposit of evaporites of the Röt Formation (Fig. S1). In total, seven gas wells were drilled in the Sleen municipality. The first exploratory well (SLN-01), drilled in 1950, was abandoned at a depth of around 1,000 m after no hydrocarbons had been encountered. SLN-02 was destroyed in the blowout, and SLN-03 was used as the relief well. Wells SLN-04 up to SLN-07 (Fig. 2) were drilled between 1975 and 1980. Gas was produced from the aforementioned Triassic sandstones of the Bundsandstein Group. However, it was found that the reservoir was highly compartmentalized due to fracturing. Hence, production was halted after only 40% of the

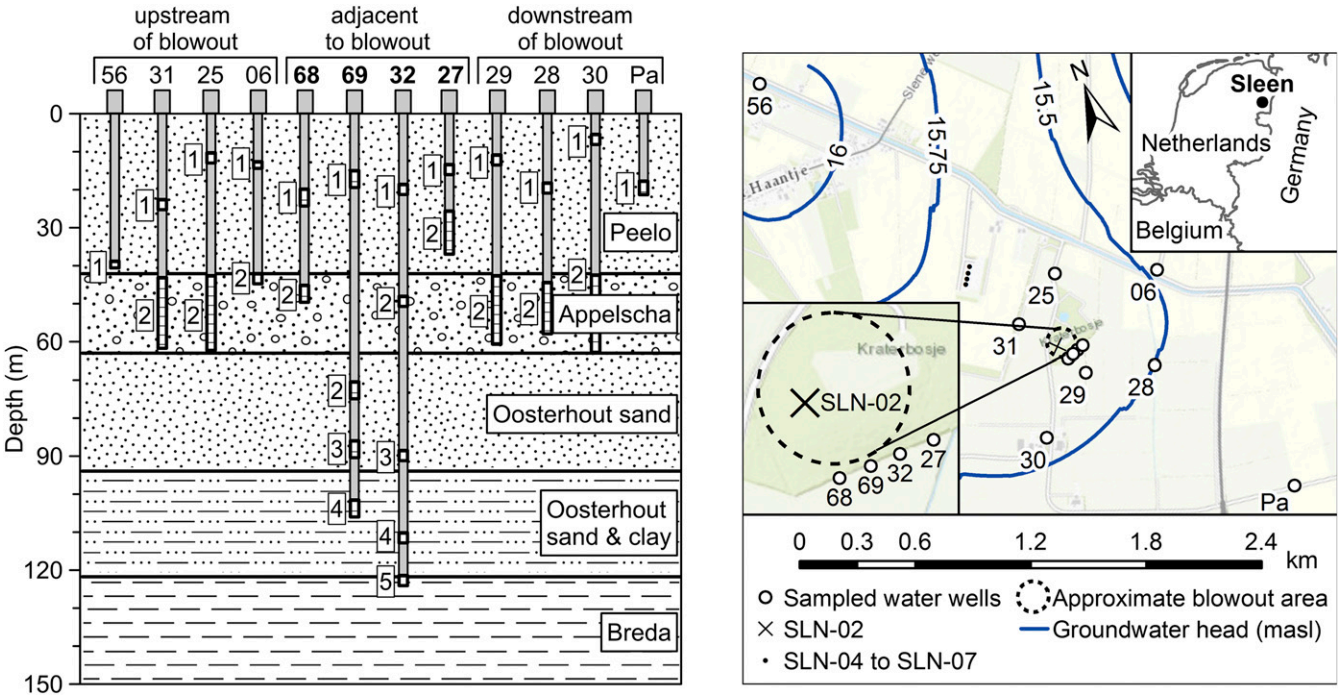

Fig. 2. (*Left*) Shallow stratigraphy showing the dominant lithology of each formation as well as the approximate location, depth, length, and designation of each wellbore and individual monitoring well. (*Right*) Topographic map showing the location of the groundwater monitoring wells sampled for this study as well as the spud point of the blowout well (SLN-02) and other nearby gas wells. Blue lines signify hydraulic head contours.

Table 1. Detailed results of the chemical analyses of sampled wells, as well as the depth of the middle of the well screen and stratigraphy

Screen ID	Depth mid-screen, mbgl	Formation	CH_4, mg/L	C1/[C2 + C3], molar ratio	δ^{13}C-CH_4, ‰ (PDB)	δD-CH_4, ‰ (SMOW)	Alkalinity, mg/L, as HCO_3	Mn, mg/L	Fe, mg/L	pH	NH_4 , mg/L	SO_4, mg/L
Pa-1	−20.0	Peelo	0.08	871	−59.6	−341	178	0.31	11.39	7.06	0.21	<1.3
06-1	−12.7	Peelo	2.6	7,923	−75.8	−259	136	0.56	17.16	6.98	2.73	<1.3
06-2	−41.2	Appelscha	4.7	5,828	−73.0	−235	111	0.63	21.41	6.76	3.14	<1.3
25-1	−12.5	Peelo	0.08	24,000	−55.9	−356	47	0.18	13.50	6.94	0.85	2.4
25-2	−56.2	Appelscha	0.02	270	−61.9	−254	54	0.22	11.13	6.09	0.86	43.1
27-1	−14.0	Peelo	14.4	44	−26.0	−98	333	0.51	44.74	6.97	0.30	<1.3
27-2	−32.0	Peelo	0.88	108	−21.3	−62	40	0.54	20.25	7.10	1.38	32.2
28-1	−19.0	Peelo	4.6	52	−15.5	−12	108	0.68	20.29	7.26	0.48	<1.3
28-2	−52.5	Appelscha	0.62	43	−15.3	−33	49	0.48	12.46	7.20	0.54	<1.3
29-1	−12.0	Peelo	9.9	35	−18.5	−65	275	0.39	26.38	6.89	2.51	<1.3
29-2	−50.0	Appelscha	16.4	44	−21.1	−112	71	0.39	14.66	6.88	0.17	34.7
30-1	−5.7	Peelo	1.9	10,500	−54.3	−260	373	0.68	41.78	6.45	0.35	<1.3
30-2	−52.8	Appelscha	0.06	1,125	−65.9	−213	52	0.24	16.78	6.89	0.45	24.8
31-1	−27.0	Peelo	0.08	112	−20.1	111	31	0.07	20.84	5.82	0.77	21.9
31-2	−55.0	Appelscha	0.01	260	−70.0		45	0.21	25.89	6.56	0.07	52.4
32-1	−20.0	Peelo	22.8	65	−20.4	−90	642	0.65	60.15	6.85	1.07	36.7
32-2	−49.0	Appelscha	13.4	80	−20.7	−106	57	0.45	8.36	7.00	0.27	23.4
32-3	−88.0	Oosterhout	32.6	34	−21.3	−117	193	0.06	2.74	7.73	0.14	<1.3
32-4	−109.0	Oosterhout	28.8	34	−21.1	−118	221	0.10	1.61	7.97	3.80	21.4
32-5	−120.0	Breda	43.8	36	−20.8	−118	244	0.09	0.68	8.38	1.01	4.1
56-1	−51.6	Peelo	0.20	523	−36.5	−195	158	0.23	9.19	7.40	0.08	32.6
68-1	−24.0	Peelo	32.2	40	−21.8	−111	209	0.18	20.95	7.39	0.21	0.0
68-2	−54.0	Appelscha	0.11	27	−48.2	−196	60	0.47	19.10	7.17	0.30	38.6
69-1	−17.5	Peelo	20.4	46	−17.7	−74	131	0.30	40.43	7.17	0.19	31.5
69-2	−72.5	Oosterhout	42.9	33	−21.2	−117	470	0.02	2.25	7.58	0.11	<1.3
69-3	−87.5	Oosterhout	32.3	32	−21.3	−118	212	0.03	2.41	7.65	0.44	<1.3
69-4	−102.5	Oosterhout	33.1	32	−21.1	−117	237	0.04	4.40	7.80	2.71	219.7

mbgl, meters below ground level; SMOW, Standard Mean Ocean Water; VPDB, Vienna Pee Dee Belemnite.

total gas in the reservoir had been produced (20). The chemical and carbon isotopic composition of gas produced from the Sleen field is available through the analyses of samples from wells SLN-04, SLN-05, and SLN-07 carried out in the early 2000s (Table S1). Notably, the average mole fraction of nitrogen in gas samples from the Sleen field is very high at 53.7%, while that of methane is 44.7%. The average δ^{13}C-CH_4 of the three samples was −22.1‰ (δD-CH_4 was not analyzed).

Results and Discussion

Minimum and maximum observed methane concentrations in the groundwater monitoring wells near the blowout were 0.01 and 43.8 mg/L, respectively (Table 1). The highest methane concentrations were found in the monitoring wells directly adjacent to the blowout area. Although no threshold levels for safe concentrations of methane in groundwater have been set in The Netherlands, methane concentrations in 12 of the sampled monitoring wells exceeded the recommended 10-mg/L hazard threshold level set by the US Department of the Interior (21). Of these 12 wells, seven exceeded the 28-mg/L hazard mitigation level. As methane concentrations up to 100 mg/L have been shown to occur naturally in Dutch groundwater (22), concentrations alone were not sufficient for determining the origin of dissolved methane. Isotopic characterization showed that all samples with concentrations greater than 10 mg/L ($n = 12$) had a δ^{13}C-CH_4 above −30‰ (Fig. 3), typical of a thermogenic origin. Biogenic methane (δ^{13}C-CH_4 < −50‰) in concentrations higher than 1 mg/L was only encountered in three monitoring wells up-gradient of the blowout (wells 06-1, 06-2, and 30-1 with concentrations of 2.6, 4.7, and 1.9 mg/L, respectively). Supporting the biogenic origin of methane in these samples are the elevated ammonium concentrations (Fig. S2), a common byproduct during methanogenic decomposition of organic matter (23).

The maximum distance at which dissolved thermogenic methane was identified is 515 m down-gradient of the location of the blowout well in both monitoring wells 28-1 and 28-2 (Fig. 2). This suggests that dissolved methane traveled with a minimum effective velocity of 10 m·y^{-1} in both the Peelo and Appelscha Formations. One kilometer further down-gradient, at monitoring

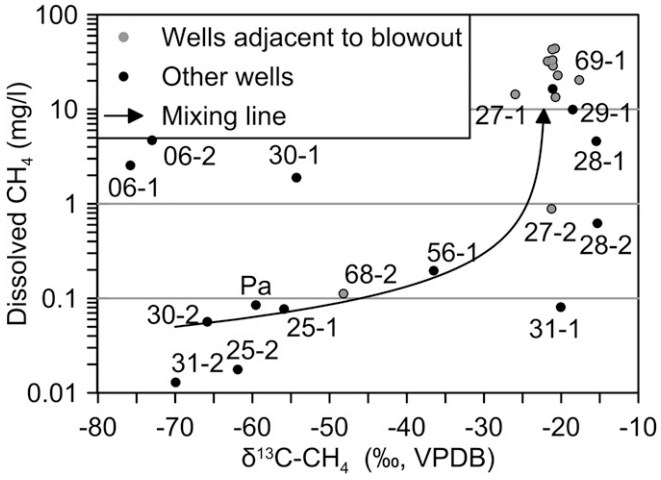

Fig. 3. Carbon isotope ratio vs. dissolved methane concentration. Samples labeled with gray dots are from the four wells located directly adjacent to the approximate location of the crater (68, 69, 32, and 27; Fig. 1). The mixing line is calculated with a biogenic end member (0.05 mg/L, −70‰) and a thermogenic end member (10 mg/L, −22‰). VPDB, Vienna Pee Dee Belemnite.

well Pa (Fig. 2), the groundwater appears to be unaffected by the blowout. However, this well is screened in the Peelo Formation and not the more conductive Appelscha Formation, where methane contamination could have traveled farther. Assuming a hydraulic conductivity of 100 $m{\cdot}d^{-1}$ and porosity of 0.3, groundwater in this formation is estimated to have an average velocity of 30 $m{\cdot}y^{-1}$, given the hydraulic head gradient of around 0.25 m/km. Methane concentrations in monitoring wells 25 and 31 (located 230 and 383 m upgradient of the blowout well, respectively) are less than 0.1 mg/L. This shows that although lateral free gas migration may have occurred during the blowout, this does not contribute significantly to the observed present-day distribution of methane concentrations. Such two-phase gas migration would be largely independent of the direction of the low hydraulic gradient, and hence occur in all directions equally.

There was no visually recognizable methane seepage at ground surface. However, the fact that methane concentrations are still highest in the wells directly adjacent to the location of the crater formed by the blowout (Fig. 3) suggests that leakage from the reservoir is still ongoing. Otherwise, with the estimated effective velocity of 30 $m{\cdot}y^{-1}$ in the Appelscha Formation, it is likely that any dissolved methane released during the blowout event would have been transported beyond the monitoring wells during the past 50 y. Also, the phreatic sandy nature of the shallow groundwater system studied precludes the conditions for secondary gas accumulations. In addition, a recent field experiment (24) in which gas-phase methane was injected into a shallow sedimentary aquifer illustrated that residual methane was dissolved on a time scale of months, not years. Alternatively, matrix diffusion of aqueous methane from the Oosterhout or Breda clays (Fig. 2) due to underlying secondary gas entrapment might be the origin of thermogenic methane in the shallow groundwater system. However, such a process would yield strictly increasing dissolved methane concentrations with depth, which is not observed (Table 1).

Hence, we argue that the most plausible explanation for the elevated concentrations of thermogenic methane found in the shallow groundwater system overlying the location of a blowout is that gas-phase methane leakage from a deeper thermogenic gas source continues to this day. Whether or not that source is the primary source from which the blowout occurred or secondarily formed gas entrapments is unknown. However, the perturbation of the sedimentary sequence due to the blowout would have negatively impacted the likelihood of secondary gas accumulations. Therefore, ongoing leakage of thermogenic

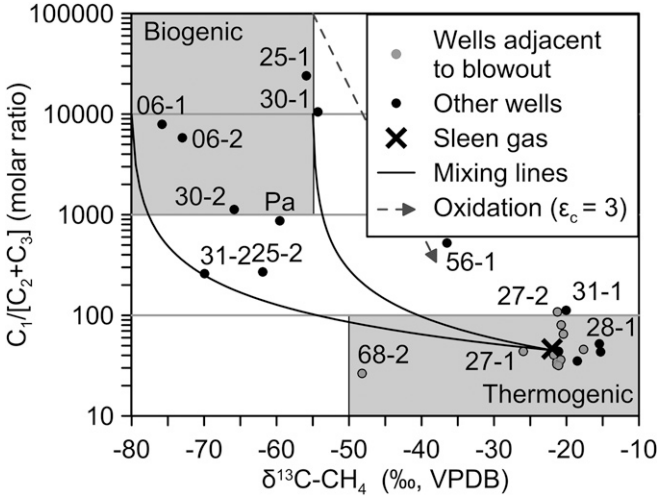

Fig. 4. $C_1/(C_2 + C_3)$ vs. $\delta^{13}C$-CH_4 of analyzed groundwater wells. Mixing lines are between a thermogenic end member (average value of the three available samples from the Sleen gas field) and two possible biogenic end members [$C_1/(C_2 + C_3)$ of 10,000 and $\delta^{13}C$ of −80‰ and −55‰]. Oxidation is calculated according to equation 15 of ref. 30. VPDB, Vienna Pee Dee Belemnite.

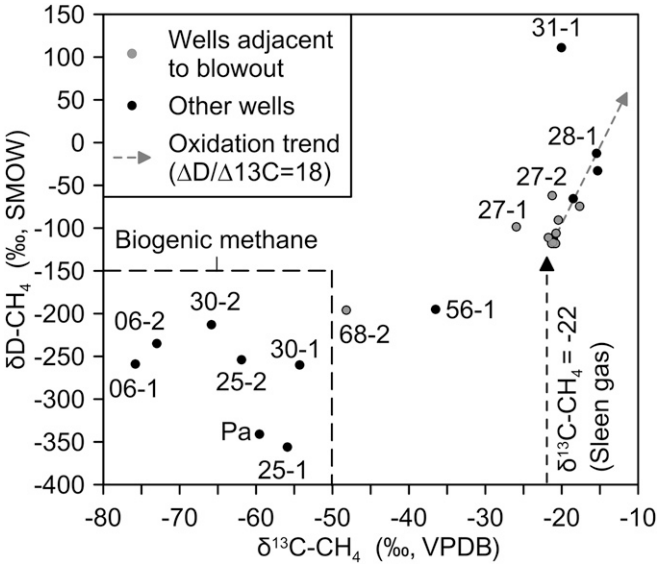

Fig. 5. $\delta^{13}C$-CH_4 vs. δD-CH_4 of analyzed groundwater wells. The gray arrow represents the calculated (according to ref. 30) isotopic enrichment due to AOM with $\varepsilon_C = 3$ and $\varepsilon_D = 54$ ($\Delta D/\Delta^{13}C = 18$). In the absence of δD-CH_4 analyses from the Sleen gas field, the black arrow shows the $\delta^{13}C$-CH_4 of Sleen gas. SMOW, Standard Mean Ocean Water; VPDB, Vienna Pee Dee Belemnite.

methane directly from the Sleen gas reservoir from which the blowout occurred is considered most likely.

The combination of molecular composition ($C_1/[C_2 + C_3]$ ratio) and the methane carbon isotope ratio found in the majority of water wells adjacent to the blowout indeed closely resembles that of the samples from the Sleen reservoir (Fig. 4). Additionally, a subset of samples fall within a range of values that can be explained by mixing of biogenic methane formed in situ with thermogenic methane from the Sleen reservoir. Higher $C_1/[C_2 + C_3]$ ratios than that of the reservoir are observed in a number of samples with thermogenic methane. This molecular fractionation could be due to the differential solubility and sorption characteristics of methane and higher alkanes (6). Such "solubility fractionation" was used to explain elevated C_1/C_2 ratios of thermogenic methane in groundwater in West Virginia (25). Alternatively, molecular fractionation may occur as a result of the preferential oxidation of nonmethane alkanes (26, 27). Partial oxidation of dissolved ethane should leave the residual ethane enriched in $\delta^{13}C$-C_2H_6, as the lighter ^{12}C is preferentially consumed. Indeed, several thermogenic samples with elevated $C_1/[C_2 + C_3]$ ratios were found to have enriched $\delta^{13}C$-C_2H_6, giving credence to this hypothesis (Fig. S3).

The relation between $\delta^{13}C$-CH_4 and δD-CH_4 indicates that a number of groundwater samples were significantly enriched in both carbon and hydrogen isotopic compositions (Fig. 5). Most notably, wells 29 and 28 (which lie directly down-gradient of the blowout well at a distance of 201 and 515 m, respectively) showed progressive isotopic enrichment along with decreasing methane concentrations, indicating degradation. Since conditions are anoxic, this enrichment is likely the result of the anaerobic oxidation of methane (AOM) (28), a process that could potentially limit the extent of a groundwater methane plume (29). Isotopic fractionation factors of methane can be quantified as a function of the amount of residual (nonoxidized) methane using the classical Rayleigh fractionation equation, which can be rewritten as follows (30):

$$\delta^{13}C(CH_4)_t = \delta^{13}C(CH_4)_i - \varepsilon_C \cdot \ln(f), \quad [1]$$

where f is the residual methane fraction, ε_C is the kinetic isotopic fractionation factor, and $\delta^{13}C(CH_4)_t$ and $\delta^{13}C(CH_4)_i$ are the carbon isotopic ratios of the residual and initial methane, respectively, and similarly for deuterium enrichment.

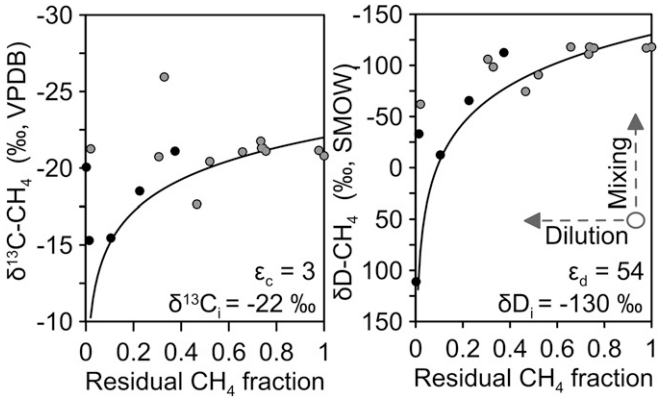

Fig. 6. Percentage of residual methane versus δ^{13}C-CH_4 (*Left*) and δD-CH_4 (*Right*). Isotopic fractionation as a result of AOM was modeled using Eq. **1**. Residual methane fractions were calculated as a function of the maximum observed methane concentration (43.8 mg/L in well 32-5). The best fit was achieved with fractionation factors of $\varepsilon_C = 3$ and $\varepsilon_D = 54$ and initial isotopic compositions of δ^{13}C-$CH_4 = -22‰$ and δD-$CH_4 = -130‰$. The four wells adjacent to the blowout are indicated with gray circles, and all other wells are indicated with black circles. SMOW, Standard Mean Ocean Water; VPDB, Vienna Pee Dee Belemnite.

Fig. 6 shows that a reasonable fit was achieved with $\varepsilon_C = 3$ and $\varepsilon_D = 54$ and an initial isotopic composition of $\delta^{13}C = -22‰$ and $\delta D = -130‰$. Due to the uncertainty in travel time of the methane toward individual well screens, as well as mixing with unknown proportions of biogenic methane, some deviation from the modeled line is expected. Calculated fractionation factors fall within the low end of the reported range for anaerobic microbial methane oxidation (30). The relatively low fractionation factors could be due, in part, to the diluting effect of dispersion on the decreasing methane concentrations during transport with groundwater flow, which does not affect the isotopic composition. In addition, however, the low fractionation factors could possibly be due to iron oxide-mediated AOM, as this oxidation pathway results in lower fraction factors than for sulfate-coupled AOM (31). The resulting ratio of carbon versus deuterium enrichment ($\Delta D/\Delta^{13}C$) was found to be 18 (Fig. 5), which falls within the wide range of values for AOM coupled to the reduction of both sulfate and iron oxides as derived from a limited amount of available studies (30–32).

Methane oxidation coupled to sulfate, iron oxides, or manganese oxides is described by the following net reactions (33), respectively:

$$CH_4 + 4MnO_2 + 7H^+ \rightarrow HCO_3^- + 4Mn^{2+} + 5H_2O \quad [2]$$

$$CH_4 + 8Fe(OH)_3 + 15H^+ \rightarrow HCO_3^- + 8Fe^{2+} + 21H_2O \quad [3]$$

$$CH_4 + SO_4^{2-} \rightarrow HCO_3^- + HS^- + H_2O \quad [4]$$

Elevated alkalinities are associated with all three pathways and were indeed encountered in a subset of wells with elevated methane concentrations (Fig. S2). While AOM coupled to sulfate reduction has frequently been described in groundwater systems (18, 28, 34), sulfate concentrations appear to be unrelated to methane concentrations (Fig. S2). Instead, both iron and manganese concentrations are elevated in wells with intermediate methane concentrations (~1–20 mg/L), indicating that the reduction of iron and manganese oxides is the predominant AOM pathway (Fig. 7). The lower iron and manganese concentrations in the wells with the highest methane concentrations in the vicinity of the blowout area show that reactive iron and manganese oxides have become depleted. These more reduced conditions might locally allow AOM coupled to sulfate reduction to become more dominant.

The depletion of iron and manganese oxides in the wells directly down-gradient from the blowout zone highlights the fact that while AOM plays an important role in controlling the fate of dissolved methane, it is ultimately limited by the initial availability of iron and manganese oxides in the aquifer sediments. As precipitation of siderite ($FeCO_3$) and rhodochrosite ($MnCO_3$) likely occurs simultaneously with reduction, using the aqueous Fe and Mn concentrations to calculate a rate of oxidation would lead to an underestimation of the actual oxidation rate (35). Increased manganese concentrations are observed at lower methane concentrations than increased iron concentrations (i.e., at the fringe of the plume). This could be due to AOM coupled to the reduction of manganese oxides being thermodynamically more favorable than AOM coupled to the reduction of iron oxides when the concentrations of the relevant aquatic species involved are nearly identical (33, 36).

Given the complexity of the biogeochemical process, interpretation in terms of zero-order or first-order degradation is inexact. Nevertheless, a tentative assessment of the rate of oxidation can be made based on the observed methane concentrations along the 515-m transect from the location of blowout well SLN-02 past monitoring wells 32-1, 29-1, and 28-1. Neglecting the influence of hydrodynamic dispersion on the attenuation of methane concentrations along this transect and assuming a flow velocity of 10 $m \cdot y^{-1}$ to each of these wells yields a rate of oxidation of 0.38 $mg \cdot L^{-1} \cdot y^{-1}$ (Fig. S4). While rates of AOM in freshwater environments are still poorly constrained, this calculated rate is much lower than the average rate of oxidation of 117 $mg \cdot L^{-1} \cdot y^{-1}$ observed in a recent study of AOM in freshwater wetlands (37). This shows that, at least theoretically, the near-complete disappearance of methane along the 500-m flow path can be attributed to AOM.

The occurrence of methane oxidation in stray gas-impacted groundwater has important implications for groundwater monitoring programs aimed at uncovering natural and anthropogenic sources of gas leakage. Here, the maximum distance down-gradient of the blowout at which thermogenic methane was detected is ~500 m and is limited by the occurrence of methane oxidation. Hence, while stray gas migration may occur over much greater distances in other hydrogeological circumstances (38), monitoring should ideally occur in close proximity to possible leakage sources. In addition, the occurrence of methane

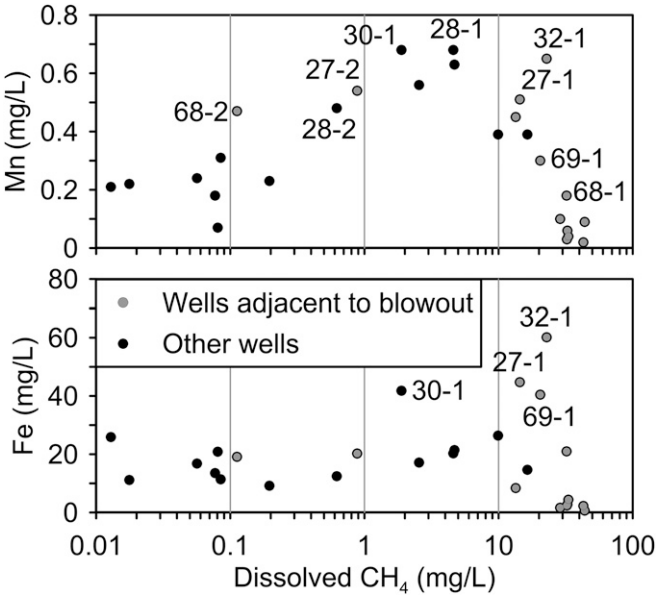

Fig. 7. Dissolved methane concentrations plotted against concentrations of manganese and iron for all sampled wells.

oxidation causes enrichment of methane isotopic composition, which could lead to false-positive detections of thermogenic methane. A good example thereof is presented by well 56-1 in this study. This well was expected to contain biogenic methane, given that it is located ∼2 km up-gradient of the blowout. In the absence of knowledge about the composition of leaked gas and local redox conditions, its $\delta^{13}C$ and δD values of −36.5‰ and −195.0‰, respectively, would typically be considered thermogenic. However, the unusual isotopic composition of methane in the water from well 56-1 is likely the result of microbial oxidation of biogenic methane (Fig. 4).

Conclusions

Fifty years after the catastrophic underground blowout that occurred near the village of Sleen, The Netherlands, a detailed investigation of the groundwater chemistry was carried out in the shallow aquifer overlying the blowout location. This study led to the following conclusions:

i) Dissolved methane concentrations in wells close to the location of the blowout are highly elevated (up to 44 mg/L) compared with those in background wells. Methane in concentrations greater than 10 mg/L is thermogenic and originates from the Sleen reservoir at 2 km below ground surface.

ii) Most likely, the long-term persistence of elevated methane concentrations adjacent to the blowout site is the result of continuing gas leakage form the Sleen reservoir initiated by the blowout.

iii) AOM coupled to the reduction of iron and manganese oxides plays a major role in the natural attenuation of the dissolved methane plume. However, the oxidation capacity is limited by the availability of iron and manganese oxides in the aquifer sediments, which is resulting in a slowly expanding methane plume.

iv) Considering the potential impact of methane oxidation, monitoring for gas contamination should be conducted in close proximity to potential gas leakage sources, and at multiple monitoring locations. Relying on single sampling points may lead to false "nondetects" if the monitoring distance is too large. In addition, the compositional and isotopic impact of oxidation may lead to erroneous assessment of the origin of dissolved gases, especially when $\delta^{13}C$ is analyzed without δD.

Materials and Methods

A total of 27 groundwater samples were collected between January and April 2016 from 12 nested and two individual groundwater monitoring wells (Fig. 2). Samples were only collected after the temperature, pH, and electrical conductivity of the water had stabilized and dissolved oxygen indicated stable anoxic conditions. Samples for the analyses of dissolved gas chemical and isotopic composition were collected using IsoFlasks and analyzed by ISOLAB for gas composition (C1 to C5, C5+, N_2, CO_2, O_2, and Ar) as well as the following stable isotope ratios: $\delta^{13}C$-CH_4, $\delta^{13}C$-C_2H_6, $\delta^{13}C$-C_3H_8, $\delta^{2}H$-CH_4, and $\delta^{13}C$-CO_2. Analytical details are given in *SI Methods*.

ACKNOWLEDGMENTS. We acknowledge the Watermaatschappij Drenthe for providing access to groundwater monitoring wells and facilitating the groundwater sampling campaign. We also acknowledge Royal Dutch Shell for providing results of the analyses of gas samples from the Sleen gas field. This work is part of the research program "Shale Gas & Water" (Project 859.14.001), which is financed by the Netherlands Organization for Scientific Research.

1. Harrison SS (1983) Evaluating system for ground-water contamination hazards due to gas-well drilling on the glaciated Appalachian plateau. *Ground Water* 21:689–700.
2. Dyck W, Dunn CE (1986) Helium and methane anomalies in domestic well waters in southwestern Saskatchewan, Canada, and their relationship to other dissolved constituents, oil and gas fields, and tectonic patterns. *J Geophys Res Solid Earth* 91: 12343–12353.
3. Osborn SG, Vengosh A, Warner NR, Jackson RB (2011) Methane contamination of drinking water accompanying gas-well drilling and hydraulic fracturing. *Proc Natl Acad Sci USA* 108:8172–8176.
4. Jackson RB, et al. (2013) Increased stray gas abundance in a subset of drinking water wells near Marcellus shale gas extraction. *Proc Natl Acad Sci USA* 110:11250–11255.
5. Darrah TH, Vengosh A, Jackson RB, Warner NR, Poreda RJ (2014) Noble gases identify the mechanisms of fugitive gas contamination in drinking-water wells overlying the Marcellus and Barnett shales. *Proc Natl Acad Sci USA* 111:14076–14081.
6. Etiope G, Feyzullayev A, Baciu CL (2009) Terrestrial methane seeps and mud volcanoes: A global perspective of gas origin. *Mar Pet Geol* 26:333–344.
7. Schroot BM, Klaver GT, Schüttenhelm RTE (2005) Surface and subsurface expressions of gas seepage to the seabed—Examples from the southern North Sea. *Mar Pet Geol* 22:499–515.
8. Gorody AW (2012) Factors affecting the variability of stray gas concentration and composition in groundwater. *Environ Geosci* 19:17–31.
9. Schwartz MO (2015) Modelling the hypothetical methane-leakage in a shale-gas project and the impact on groundwater quality. *Environ Earth Sci* 73:4619–4632.
10. Chilingar GV, Endres B (2005) Environmental hazards posed by the Los Angeles Basin urban oilfields: An historical perspective of lessons learned. *Environ Geol* 47:302–317.
11. Davies RJ, Mathias SA, Moss J, Hustoft S, Newport L (2012) Hydraulic fractures: How far can they go? *Mar Pet Geol* 37:1–6.
12. Jackson RB, et al. (2014) The environmental costs and benefits of fracking. *Annu Rev Environ Resour* 39:327–362.
13. Tingay MRP, Hillis RR, Morley CK, Swarbrick RE, Drake SJ (2005) Present-day stress orientation in Brunei: A snapshot of "prograding tectonics" in a Tertiary delta. *J Geol Soc London* 162:39–49.
14. Patterson LA, et al. (2017) Unconventional oil and gas spills: Risks, mitigation priorities, and state reporting requirements. *Environ Sci Technol* 51:2563–2573.
15. Hsieh PA (2011) Application of MODFLOW for oil reservoir simulation during the Deepwater Horizon crisis. *Ground Water* 49:319–323.
16. Conley S, et al. (2016) Methane emissions from the 2015 Aliso Canyon blowout in Los Angeles, CA. *Science* 351:1317–1320.
17. Grace RD (2003) *Blowout and Well Control Handbook* (Gulf Professional Publishing, Houston).
18. Kelly WR, Matisoff G, Fisher JB (1985) The effects of a gas well blow out on groundwater chemistry. *Environ Geol Water Sci* 7:205–213.
19. Vernes RW, van Doorn TH (2005) *Van Gidslaag naar Hydrogeologische Eenheid; Toelichting op de totstandkoming van de dataset REGIS II* (TNO, Utrecht, The Netherlands), NITG-05-038-B. Dutch.
20. Nederlandse Aardolie Maatschappij B.V. (2003) Winngsplan Zuid-Oost Drenthe (NAM, Assen, The Netherlands). Available at https://goo.gl/VzqL4a. Accessed April 5, 2017.
21. Eltschlager KK, Hawkins JW, Ehler WC, Baldassare FJ (2001) *Technical Measures for the Investigation and Mitigation of Fugitive Methane Hazards in Areas of Coal Mining* (US Department of the Interior Office of Surface Mining, Reclamation, and Enforcement, Pittsburgh), p 129.
22. Fortuin NPM, Willemsen A (2005) Exsolution of nitrogen and argon by methanogenesis in Dutch ground water. *J Hydrol (Amst)* 301:1–13.
23. Griffioen J, Vermooten S, Janssen G (2013) Geochemical and palaeohydrological controls on the composition of shallow groundwater in the Netherlands. *Appl Geochem* 39:129–149.
24. Cahill AG, et al. (2017) Mobility and persistence of methane in groundwater in a controlled-release field experiment. *Nat Geosci* 10:289–294.
25. Harkness JS, et al. (2017) The geochemistry of naturally occurring methane and saline groundwater in an area of unconventional shale gas development. *Geochim Cosmochim Acta* 208:302–334.
26. Sassen R, et al. (2004) Free hydrocarbon gas, gas hydrate, and authigenic minerals in chemosynthetic communities of the northern Gulf of Mexico continental slope: Relation to microbial processes. *Chem Geol* 205:195–217.
27. Musat F (2015) The anaerobic degradation of gaseous, nonmethane alkanes–From in situ processes to microorganisms. *Comput Struct Biotechnol J* 13:222–228.
28. Van Stempvoort D, Maathuis H, Jaworski E, Mayer B, Rich K (2005) Oxidation of fugitive methane in ground water linked to bacterial sulfate reduction. *Ground Water* 43:187–199.
29. Roy N, Molson J, Lemieux JM, Van Stempvoort D, Nowamooz A (2016) Three-dimensional numerical simulations of methane gas migration from decommissioned hydrocarbon production wells into shallow aquifers. *Water Resour Res* 52:5598–5618.
30. Whiticar MJ (1999) Carbon and hydrogen isotope systematics of bacterial formation and oxidation of methane. *Chem Geol* 161:291–314.
31. Egger M, et al. (2015) Iron-mediated anaerobic oxidation of methane in brackish coastal sediments. *Environ Sci Technol* 49:277–283.
32. Coleman DD, Risatti JB, Schoell M (1981) Fractionation of carbon and hydrogen isotopes by methane-oxidizing bacteria. *Geochim Cosmochim Acta* 45:1033–1037.
33. Beal EJ, House CH, Orphan VJ (2009) Manganese- and iron-dependent marine methane oxidation. *Science* 325:184–187.
34. Timmers PH, et al. (2016) Anaerobic oxidation of methane associated with sulfate reduction in a natural freshwater gas source. *ISME J* 10:1400–1412.
35. van Breukelen BM, Griffioen J, Röling WFM, van Verseveld HW (2004) Reactive transport modelling of biogeochemical processes and carbon isotope geochemistry inside a landfill leachate plume. *J Contam Hydrol* 70:249–269.
36. Stumm W, Morgan JJ (1996) *Aquatic Chemistry: Chemical Equilibria and Rates in Natural Waters* (Wiley, New York).
37. Segarra KEA, et al. (2015) High rates of anaerobic methane oxidation in freshwater wetlands reduce potential atmospheric methane emissions. *Nat Commun* 6:7477.
38. Llewellyn GT, et al. (2015) Evaluating a groundwater supply contamination incident attributed to Marcellus shale gas development. *Proc Natl Acad Sci USA* 112: 6325–6330.
39. Cirkel G, Hartog N, De La B, Gonzalez L, Stuyfzand P (2015) Methaan in ondiep Nederlands grondwater: Verbinding met de diepe ondergrond? Available at https://goo.gl/7GCtkS. Accessed August 25, 2016. Dutch.